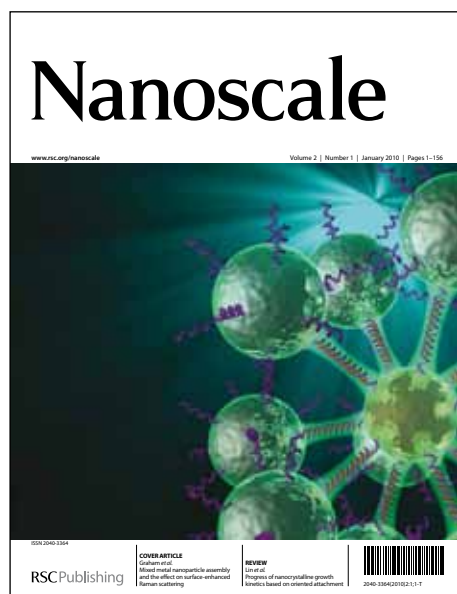


Nanoscale

Accepted Manuscript



This is an *Accepted Manuscript*, which has been through the RSC Publishing peer review process and has been accepted for publication.

Accepted Manuscripts are published online shortly after acceptance, which is prior to technical editing, formatting and proof reading. This free service from RSC Publishing allows authors to make their results available to the community, in citable form, before publication of the edited article. This *Accepted Manuscript* will be replaced by the edited and formatted *Advance Article* as soon as this is available.

To cite this manuscript please use its permanent Digital Object Identifier (DOI®), which is identical for all formats of publication.

More information about *Accepted Manuscripts* can be found in the [Information for Authors](#).

Please note that technical editing may introduce minor changes to the text and/or graphics contained in the manuscript submitted by the author(s) which may alter content, and that the standard [Terms & Conditions](#) and the [ethical guidelines](#) that apply to the journal are still applicable. In no event shall the RSC be held responsible for any errors or omissions in these *Accepted Manuscript* manuscripts or any consequences arising from the use of any information contained in them.

1 The role of metal layers in the formation of metal/silicon 2 hybrid nanoneedle arrays

3 Author:

4 Hai Liu¹, Chee Ying Khoo¹, Boluo Yadian¹, Qing Liu¹, Chee Lip Gan¹, Xiaohong Tang²,
5 Yizhong Huang^{1,3}

6 ¹School of Materials Science and Engineering, Nanyang Technological University 50 Nanyang
7 Avenue, 639798 (Singapore)

8 ²School of Electrical and Electronics Engineering, Nanyang Technological University 50
9 Nanyang Avenue, 639798 (Singapore)

10 Email: YZHuang@ntu.edu.sg

11

12 Abstract

13 We investigated the nanoneedle arrays fabricated on a series of metal/silicon substrates using
14 Ga⁺ ion beam patterning. It is shown that the low sputter rate metal preserves on the tip of
15 each nanoneedle in the form of gallium alloyed nanodot. The generated nanodot was found to
16 be able to greatly alleviate the ion sputtering of underlying materials. These protective metals
17 are promising to act as a shelter for the functional layer which is vulnerable from ion beam
18 irradiation. As an example reported in the present work, a bundle of GaAs nanowhiskers were
19 successfully grown on each gold nanodot protected by iron/gallium alloy.

20 1. Introduction

21 One-dimensional (1D) nanostructure array is currently an attractive area of research, and
22 many corresponding approaches or new design of nanodevices have been explored to exhibit
23 unique properties over bulk materials. Particularly, various types of high aspect ratio
24 metal/semiconductor hybrid nanostructure arrays have been investigated due to their excellent
25 performance in respective applications, *e.g.* Pt/Si/Ag nanowires for photocatalyst,¹ whiskered
26 Au/Si nanowires or Pt/Si nanoneedle for ionization gas sensing,^{2,3} Pt/Si nanowires array as
27 photoelectrode of solar cells⁴ and Fe/GaAs nanoneedle array for data storage.⁵ At present, 1D

³ Author to whom any correspondence should be addressed.

Submitted to Nanoscale

1 nanostructure arrays are produced mainly by bottom-up technique. For example, vapor-liquid-
2 solid growth of nanowire array uses dispersed metallic particles as catalyst.^{6, 7} There is an
3 alternative top-down method by selective dry or wet etching, which takes advantage of a
4 template or mask to pattern the coated substrate.⁸⁻¹⁰ When two or more materials are
5 introduced into the hybrid structure, the complexity of process integration increases
6 significantly.^{11, 12} It is therefore crucial to have more straightforward, higher efficient but less
7 time consuming procedures allowing the design and fabrication of nanostructure array
8 prototype before bulk production. Fortunately, due to the capability to assemble ordered
9 nanostructure array of high aspect ratio with mask free, focused ion beam (FIB) system is
10 prevalently utilized to produce well-aligned nanostructure array. The previous FIB researches
11 are mainly based on III-V compounds, such as GaAs⁵ or GaSb substrate,^{13, 14} and InSb/GaAs¹⁵
12 or InAs/InP heterostructure.¹⁶ The mechanism of the formation of these hybrid nanostructures
13 are generally proposed based on their high sputter rate along with low-melting-point metal
14 (indium or gallium). These liquid metals with the presence of ion irradiation are decomposed
15 from the substrate and organized as self-sustained mask.^{13-15, 17}

16 For silicon substrate, the reported investigations on FIB etching emphasize the removed
17 volume to estimate the milling yield, rather than the nanostructured surface profile.¹⁸⁻²¹ The
18 ridges or nanodots are formed around the trench banks and proposed due to the redeposition
19 or swelling effect during ion milling.^{18, 22, 23} We reported a hybrid nanostructure consisting of
20 a nanodot and nanoneedle that shows excellent gas sensitivity.²⁴ However, the role of metal
21 layers played in the formation of metal/silicon hybrid nanoneedles array has not been
22 sufficiently explored. The clarification of this will allow the creation of a criterion to control
23 the production of the ordered hybrid nanoneedles by choosing surface metals.

24 In this work, a series of metal thin layers is deposited on silicon wafer, including Ti, Cr, Co,
25 Zn, Mo, Ag, In, Sn, Hf, Ta, W, Au and Bi as hetero-substrate. The evolution of nanodots
26 formation subject to gradually increasing ion irradiation dose has been monitored by *in-situ*

1 scanning electron microscope (SEM). After that, their capabilities of nanodot formation on
2 each nanoneedle under mesh patterning have been examined respectively. Based on the
3 results, we propose the criterion of metals on silicon to achieve the hybrid nanoneedle arrays.
4 Nanowhiskers grown on ordered nanoneedle array, which require metal nanodots as catalyst,
5 have been shown as an example of its application.

6 **2. Experiment**

7 Fig. 1a shows a bright field transmission electron microscopy (TEM) image showing a
8 chromium metal layer coated on a silicon substrate, as confirmed by the energy dispersive X-
9 ray (EDX) mapping (see the inset in Fig. 1a). The metal layer was deposited by physical
10 vapor deposition (PVD) on the polished silicon surface, where a SiO₂ layer with thickness of
11 ~3nm measured in TEM is visible due to the oxidation of silicon in ambient air. Previous
12 studies on surface sputter rates of various metal/silicon material systems are quite limited.
13 Therefore, this work is focused on the observation of the gradual topographic change of
14 silicon surfaces coated with various metal under increasing perpendicular incident 30 keV
15 Ga⁺ ion dose. Fig.1b (original Si), Fig. 1c (Cr/Si) and Fig. 1d (Au/Si) are three secondary
16 electron images captured by an *in-situ* SEM at an inclined angle of 52°. Compared to Fig.1b
17 taken from the surface of the pure silicon substrate, Fig.1c appears a lot of droplets formed
18 during Ga⁺ ion irradiation, which are partially responsible by the relatively low sputter rate
19 metal of chromium.²⁵ Even the ion cascade is sufficient to form the ridge, these spherical
20 droplets still keep in place. In contrast, the gold metal, which has a higher sputter rate, is
21 subjected to the rapid removal from the surface of silicon substrate with litter meshing ion
22 dose (Fig. 1d). The responses of other types of metal/silicon substrate in ion milling are listed
23 as a matrix in supporting information (Fig S1 and S2), along with a table of their respective
24 sputter rate.²⁶⁻²⁸ Based on the data from the table, the formation of hybrid nanoneedle arrays
25 can be controlled by choosing the type of coating metal with suitable sputter rate.

26 **3. Results and discussion**

Submitted to Nanoscale

1 Fig. 2a shows the representative accomplished nanonipple array formed on the surface of
2 Cr/Si substrate, by using the previous method reported in the literatures.^{3,5, 16, 24} To optimize
3 the milling efficiency at beam current of 2.8 nA, the periodic space for the adjacent
4 nanoneedle is set to be 700 nm, which is implemented by the setting of mesh pattern
5 dimension. To investigate the microstructures using TEM, a single nanoneedle is chosen from
6 the array for the preparation of a membrane through the lift-out method in the FIB system.^{29,}
7 ³⁰ As an example, Fig. 2b shows a bright field TEM image of a single nanonipple. This
8 metal/silicon nanonipple structure is seen to consist of a featureless nanodot sitting on the top
9 of the nanoneedle. This nanodot is chromium alloyed with gallium (suggested from the EDX
10 mapping shown in Fig. 2c). It is determined to be amorphous by the fast Fourier transform
11 (FFT as inset in Fig. 2b) of its high resolution image and has a radius measured to be
12 approximately 30 nm. Nevertheless, the amorphous layer covered on the sidewall of silicon
13 nanoneedle is caused by redeposition from the substrate during ion sputtering or direct
14 amorphization induced by ion beam bombardment.^{22, 24} In contrast, the metal layer with
15 relatively higher sputter rate fails to protect the nanodots on the top from being sputtered off,
16 which leads to a pure silicon nanorod similar to that formed from the original silicon substrate,
17 as shown in Fig. 2d. The nanonipple microstructures originating from other metal/silicon
18 systems are selectively exhibited in Fig. S3, which demonstrate similar feature and elemental
19 distribution accordingly.

20 It is well accepted that the formation of nanostructure by ion milling depends on both the
21 target material system and incident beam parameters.^{18, 20-23, 25, 31} Two beam parameters were
22 tested with the formed patterns shown in Fig. S4, where the nanodots fail to be preserved
23 during ion irradiation. Each pixel of Ga⁺ focused ion beam is assumed to be subjected to a
24 two-dimensional Gaussian distribution of current density, governed by

25
$$J = \frac{I}{2\pi\sigma^2} \exp\left(-\frac{r^2}{2\sigma^2}\right) [Am^{-2}]$$

1 where J is the current density, I the incident beam current, r the distance from the analyzed
2 point to the beam center and σ the statistic deviation, which is correlated to the probe size.^{18,20}
3 In the case with a beam current of 2.8 nA, the Gaussian deviation estimated by the FIB system
4 is 66 nm, while we presume that the beam tail radius is 5σ ($\pm 0.5\sigma$) in the range of nanodots,²⁰
5 as shown in Fig 3a. The local ion dose projected to the center of nanodot from tail is in 10^{19}
6 cm^{-2} order of magnitude. Previous work reported that the dose density irradiated to substrate
7 has to be higher than 10^{17} cm^{-2} , in order to sputter silicon off rather than swell by
8 amorphization.^{23, 25, 31} This estimation is consistent with the experimental result shown in Fig.
9 2d, a blunt nanoneedle formed on pure silicon substrate with no any metal layer coated. In
10 contrast, the low-sputter-rate metal coated silicon substrate appears a hybrid structure, the
11 evolution of which is schematically outlined in Fig. 3b-d. During the ion bombardment of
12 Gaussian beam, many metal particles generated in the vicinity of high dose area are sputtered
13 out which are subsequently redeposited to the edges of the trenches, forming ridges by
14 alloying with the incident gallium ions.^{19, 22, 24} However, the as-coated metal layer is too thin
15 to stop the incident beam ions entering the c-Si substrate across the original a-Si layer.²⁵ Thus,
16 the interaction with ions in the interface between a-Si and c-Si leads to the further uniform
17 amorphization of c-Si (Fig. 2b). With more ion dose, the trench opening pushes these
18 nanodroplets moving from the pillar corners towards the center of each nanorod. This
19 coalescence procedure was ever *in-situ* observed as an “X shaped” pattern in Ref. 24, which
20 enables a thicker layer to buffer, absorb or even scatter the incident ions, as illustrated in Fig.
21 3c. Along with additional ion dose of meshing, the metallic nanodot is tapered rather than
22 piled up. At this stage, the shrinking alloyed nanodot shelters a gradually decreasing region
23 towards the center of each nanoneedle, which is responsible to the large curvature and high
24 aspect ratio, as shown in Fig. 3d.

25 The survival of silicon/metal interface by means of alloyed nanodots formation suggests that
26 the selected metal coating may protect the fragile functional film which is vulnerable to ion

Submitted to Nanoscale

1 bombardment process. For example, gold particles that act as catalyst are critical for the
2 growth of various nanowires.^{6, 7} However, due to their extremely high sputter rate, it is
3 challenging to assemble them ordered by ion beam patterning. Especially in the case of the
4 high aspect ratio structures which require excessive ion milling, the preservation of gold
5 becomes more difficult. A failed example is shown in Fig. 1c.

6 In order to solve this problem, a protective layer of iron is superimposed on gold film, as
7 illustrated in Fig. 4a. With the same meshing treatment above, a hybrid nanoneedle structure
8 array is fabricated, of which the topography is similar to Cr/Si. To investigate the
9 microstructure, a high resolution bright field TEM image of one typical nanodot is taken and
10 shown in Fig. 4b. This nanodot consists of a dark core (gold) in contrast to a slightly brighter
11 thin shell (iron-gallium alloy) as confirmed by EDX mapping in Fig. 4c. We believe that
12 during ion patterning, the alloyed iron subject to incident gallium ions will diffuse around
13 rather than rest above the gold layer, as schematically illustrated from the survived amorphous
14 silicon (Fig. 3b-d) and *in-situ* TEM observation of nanoneedles evolution (Fig. S5). This thin
15 iron layer covers the entire gold nanodot and preserves it from the further ion sputtering, in
16 particular, its sidewalls as they suffer higher sputter rate due to the angle effect.^{19-22, 25, 31} The
17 successful formation of hybrid gold/silicon nanoneedle array allows other semiconductor
18 nanowires (such as gallium arsenide) to be grown on the top of each nanoneedle, where the
19 gold nanodot acts as catalyst. The growth of GaAs nanowires was performed in the ambient
20 hydrogen of 10 mbar at 430 °C for 5 minutes. The precursor with V/III ratio of 14.2 was used
21 and GaAs nanowhiskers grown on the tip of nanoneedles as visible (Fig. 4d). No such
22 nanowhiskers were found to grow on the surface of original iron-covered gold/silicon
23 substrate. These nanowhiskers have a very small diameter of lower than 10 nm. Along with
24 their controllable high aspect ratio, they are ideal hybrid structure for the application in the
25 electric field emission or ionization.^{2, 32, 33} Meanwhile, this selective growth of nanostructures

1 is very useful and able to implement the precise assembly of 1D nanomaterial at the defined
2 area.

3 **4. Conclusion**

4 In conclusion, the metal layers play a very important role in the formation of metal/silicon
5 hybrid nanoneedle arrays in focused ion beam system. By clarification of the nanoneedle
6 structures fabricated in various metal/silicon material systems, it is proved that the low-
7 sputter-rate metal may overcome the ion bombardment by alloying with incident gallium, and
8 protect the underlayer against sputtering. One application for this capability is demonstrated
9 by preservation of vulnerable gold nanoparticle for subsequent nanowhiskers growth. Based
10 on this convenient, controllable and ubiquitous methodology, the patterning through
11 straightforward Ga ion bombardment can be further applied to a wider range of functional
12 materials, including those that are friability to ion.

13

14 **Acknowledgement:**

15 This research was supported by Tier 1 (AcRF grant MOE Singapore: RG47/11) and SUG
16 (Start-up funding in NTU: COE_SUG/RSS_20AUG10_11/14).

17

1

2

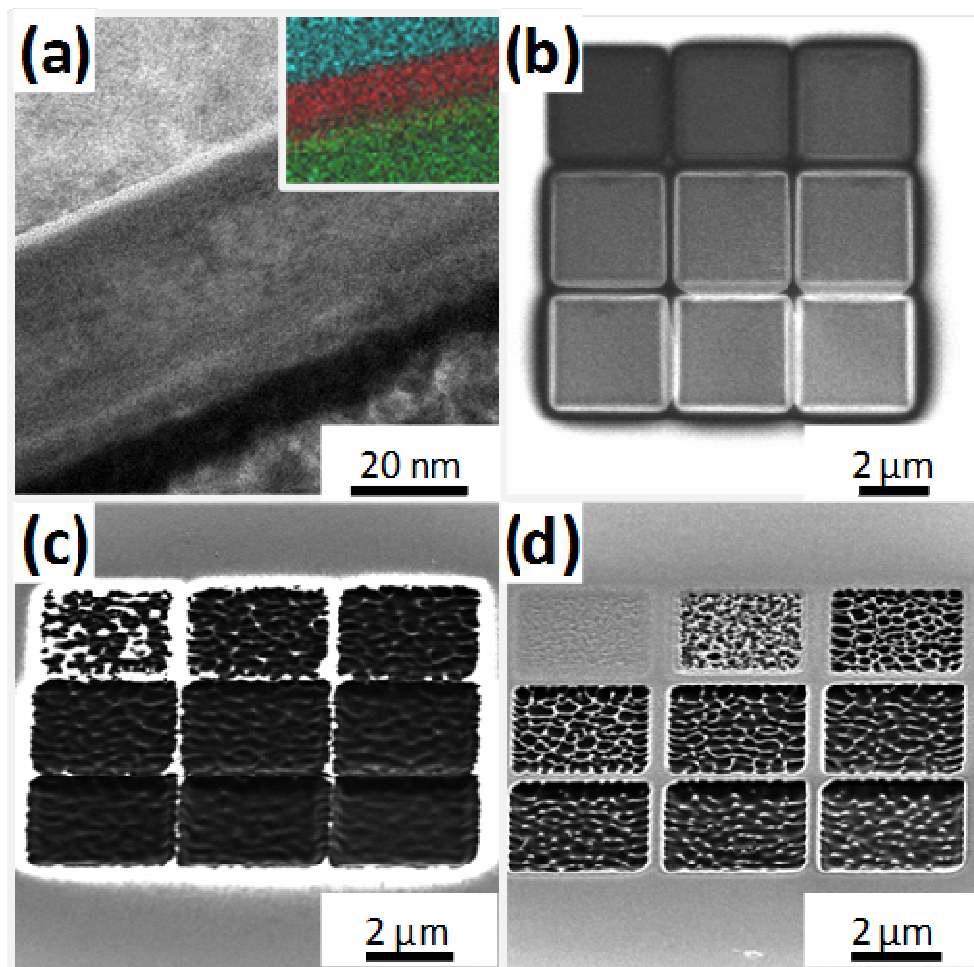
References:

- 3 1. Y. Q. Qu, L. Liao, R. Cheng, Y. Wang, Y. C. Lin, Y. Huang and X. F. Duan, *Nano*
4 *Lett*, 2010, **10**, 1941-1949.
- 5 2. R. B. Sadeghian and M. S. Islam, *Nat. Mater.*, 2011, **10**, 135-140.
- 6 3. H. Liu, B. Yadian, Q. Liu, C. L. Gan and Y. Z. Huang, *Nanotechnology*, 2013, **24**,
7 175301.
- 8 4. K. Q. Peng, X. Wang, X. L. Wu and S. T. Lee, *Nano Lett*, 2009, **9**, 3704-3709.
- 9 5. Y. Z. Huang, D. J. H. Cockayne, J. Ana-Vanessa, R. P. Cowburn, S. G. Wang and R.
10 C. C. Ward, *Nanotechnology*, 2008, **19**, 015303.
- 11 6. M. Kirkham, X. D. Wang, Z. L. Wang and R. L. Snyder, *Nanotechnology*, 2007, **18**,
12 365304.
- 13 7. P. Kratzer, S. Sakong and V. Pankoke, *Nano Lett*, 2012, **12**, 943-948.
- 14 8. M. A. Green, J. H. Zhao, A. H. Wang, P. J. Reece and M. Gal, *Nature*, 2001, **412**,
15 805-808.
- 16 9. Y. F. Huang, S. Chattopadhyay, Y. J. Jen, C. Y. Peng, T. A. Liu, Y. K. Hsu, C. L. Pan,
17 H. C. Lo, C. H. Hsu, Y. H. Chang, C. S. Lee, K. H. Chen and L. C. Chen, *Nat*
18 *Nanotechnol*, 2007, **2**, 770-774.
- 19 10. C. H. Hsu, H. C. Lo, C. F. Chen, C. T. Wu, J. S. Hwang, D. Das, J. Tsai, L. C. Chen
20 and K. H. Chen, *Nano Lett*, 2004, **4**, 471-475.
- 21 11. A. L. M. Reddy, M. M. Shaijumon, S. R. Gowda and P. M. Ajayan, *Nano Lett*, 2009,
22 **9**, 1002-1006.
- 23 12. S. Chanyawadee, R. T. Harley, M. Henini, D. V. Talapin and P. G. Lagoudakis, *Phys*
24 *Rev Lett*, 2009, **102**, 077402.
- 25 13. S. Le Roy, E. Barthel, N. Brun, A. Lelarge and E. Sondergard, *J Appl Phys*, 2009, **106**,
26 094308.
- 27 14. S. Le Roy, E. Sondergard, I. S. Nerbo, M. Kildemo and M. Plapp, *Phys Rev B*, 2010,
28 **81**.
- 29 15. J. H. Wu and R. S. Goldman, *Appl Phys Lett*, 2012, **100**, 053103.
- 30 16. K. A. Grossklaus and J. M. Millunchick, *Nanotechnology*, 2011, **22**, 355302.
- 31 17. Q. M. Wei, J. Lian, W. Lu and L. M. Wang, *Phys Rev Lett*, 2008, **100**, 076103.
- 32 18. A. A. Tseng, I. A. Insua, J. S. Park and C. D. Chen, *J Micromech Microeng*, 2005, **15**,
33 20-28.
- 34 19. A. A. Tseng, *Small*, 2005, **1**, 924-939.
- 35 20. F. Itoh, A. Shimase and S. Haraichi, *J Electrochem Soc*, 1990, **137**, 983-988.
- 36 21. H. B. Kim, G. Hobler, A. Steiger, A. Lugstein and E. Bertagnolli, *Nanotechnology*,
37 2007, **18**, 245303.
- 38 22. A. A. Tseng, *J Micromech Microeng*, 2004, **14**, R15-R34.
- 39 23. C. Lehrer, L. Frey, S. Petersen and H. Ryssel, *J Vac Sci Technol B*, 2001, **19**, 2533-
40 2538.
- 41 24. H. Liu, J. S. Wu, Y. Wang, C. L. Chow, Q. Liu, C. L. Gan, X. H. Tang, R. S. Rawat,
42 O. K. Tan, J. Ma and Y. Z. Huang, *Small*, 2012, **8**, 2807-2811.
- 43 25. L. Frey, C. Lehrer and H. Ryssel, *Appl Phys a-Mater*, 2003, **76**, 1017-1023.
- 44 26. J. Orloff, M. Utlaut and L. Swanson *High Resolution Focused Ion Beams: FIB And its*
45 *Applications*, Kluwer Academic, New York, 2002, chapter 4, 137.
- 46 27. Y. Yamamura and H. Tawara, *Atom Data Nucl Data*, 1996, **62**, 149-253.
- 47 28. In situ real-time atomic scale nanostructural synthesis, characterization and modeling,
48 <http://www.asu.edu/clas/csss/NUE/FIBSputterCalcYamamura>.
- 49 29. Y. Z. Huang, S. G. Wang, C. Wang, Z. B. Xie, D. J. H. Cockayne and R. C. C. Ward,
50 *Appl Phys Lett*, 2006, **88**, 103104.

- 1 30. N. I. Kato, Y. Kohno and H. Saka, *J Vac Sci Technol A*, 1999, **17**, 1201-1204.
- 2 31. A. Lugstein, B. Basnar, J. Smoliner and E. Bertagnolli, *Appl Phys a-Mater*, 2003, **76**,
- 3 545-548.
- 4 32. Z. Y. Hou, H. Liu, X. Wei, J. H. Wu, W. M. Zhou, Y. F. Zhang, D. Xu and B. C. Cai,
- 5 *Sensor Actuat B-Chem*, 2007, **127**, 637-648.
- 6 33. Z. Y. Hou, B. C. Cai and H. Liu, *Appl Phys Lett*, 2009, **94**, 163506.
- 7

1

2 Fig. 1

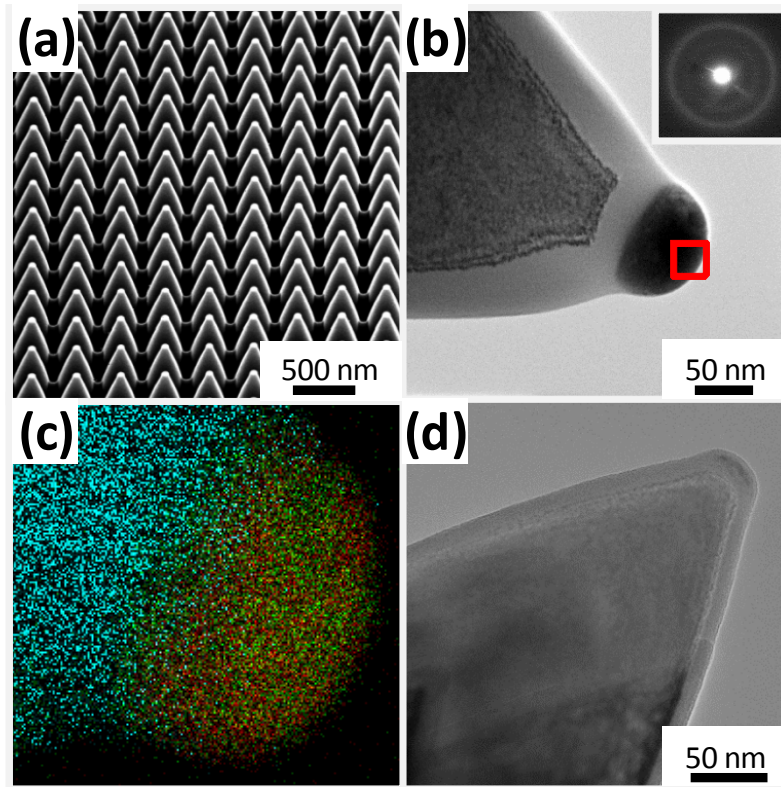


3

4 Fig. 1 (a) A bright field TEM image showing the silicon substrate coated by a chromium layer,
5 confirmed by the inset of EDX element map (red: Cr, green: Pt and cyan: Si), and the surface
6 evolution of (b) original silicon, (c) gold and (d) chromium, as a function of increasing ion
7 irradiation dose (left to right, top to bottom).

8

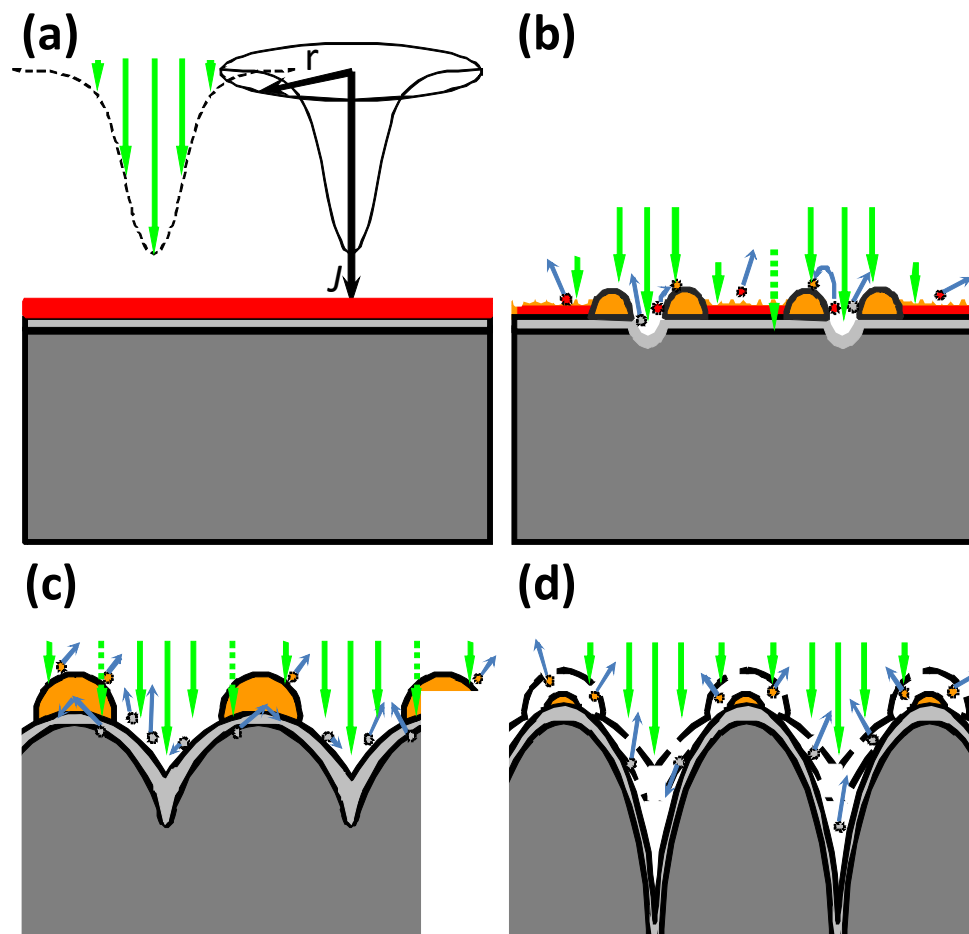
1
2 Fig. 2



3
4 Fig. 2 (a) A hybrid nanoneedle array fabricated on Cr/Si substrate, (b) A single hybrid
5 nanoneedle, where a chromium/gallium alloy nanodot sitting on the top of silicon nanoneedle
6 is identified to be amorphous by the inset FFT taken from the chosen square region. (c)
7 Elemental distribution of (b) (red: Cr, green: Ga and cyan: Si) and (d) A bright field TEM
8 image of a single blunt nanoneedle of pure silicon substrate without metallic coating.

9

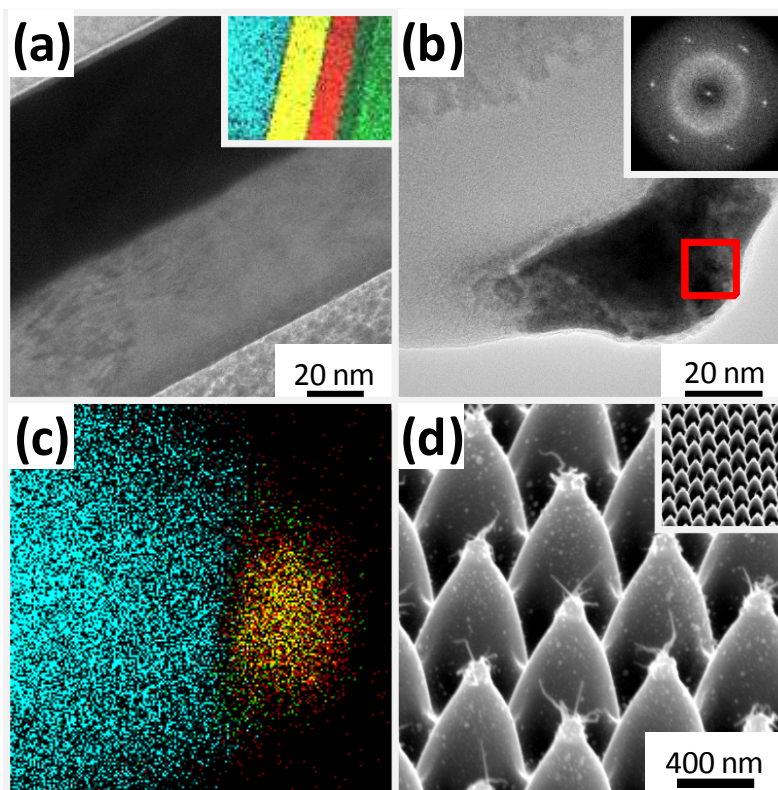
1
2 Fig. 3



3
4 Fig. 3 Schematic diagrams showing an evolution of hybrid nanoneedle formation: (a)
5 Irradiation of Gaussian ion beams (green) on a metal (red) coated silicon substrate. (b) The
6 ion beam cut through the metal and amorphous layer (bright grey) of silicon producing
7 metallic (red) and silicon (grey) particles. They mix with gallium forming an alloy (orange).
8 (c) The alloy nanodots shelter the sputtering of the underlying Si whilst the Si between
9 nanodots undergoes rapid removal. (d) Additional ions taper the metallic nanodot and silicon
10 nanoneedle leading to a high aspect ratio.

11

1
2 Fig. 4



3
4 Fig. 4 (a) A bright field TEM image of Fe/Au/Si substrate with EDX element mapping as
5 inset (green: Pt, red: Fe, yellow: Au and cyan: Si), (b) The tip of one single nanoneedle where
6 there is a metallic nanodot consisting of crystalline grains, confirmed by the inset FFT taken
7 from the selected square area, (c) EDX element mapping showing that the metallic nanodot is
8 iron-coated gold particle (green: Ga, red: Fe, yellow: Au and cyan: Si) and (d) Bundles of
9 GaAs nanowhiskers grown on the tip of hybrid nanoneedle array. The inset shows the same
10 nanoarray with a lower magnification.

A metal layer plays a key role in the formation of hybrid nanostructures consisting of nanodots on top of nanoneedles

